

Heat transfer during bubble shrinking in saturated He II under microgravity condition

S.Takada¹, N. Kimura², M. Murakami³, and T. Okamura²

¹ National Institute for Fusion Science
Oroshi-cho, Toki, Gifu, 509-5292, Japan

² High Energy Accelerator Research
1-1 Oho, Tsukuba, Ibaraki, 305-0801, Japan

³ University of Tsukuba
1-1 Tennodai, Tsukuba, Ibaraki 305-8573, Japan

takada.suguru@LHD.nifs.ac.jp

Abstract. Microgravity experiments of He II boiling were carried out using a drop tower. The process of bubble shrinking in He II in microgravity was observed by a high speed camera. The time duration of the microgravity environment less than 1 mg was about 1.3 sec. First, a large spherical bubble of about 10 mm in diameter was created by a short wire heater (Diameter 0.05 x Length 2.82 mm) for a heating time of 0.4 sec. The subsequent bubble shrinking was visualized after the heater was switched off. The time variation of the volume of bubble was estimated by image analysis. The shrinking speed of bubble was calculated from these time variation data. The shrinking speed depends on the heat flux across the liquid-vapor interface. It is found that the heat flux across the interface in microgravity can be explained by the kinetic theory with a pressure difference due to surface tension.

1. Introduction

Superfluid helium (He II) has been utilized in space applications. Thus, the study of the boiling heat transfer in He II under a microgravity condition was required. Our group has carried out the experimental studies using drop tower [1-4]. One of the important issues is the critical heat flux of the onset boiling in He II under microgravity conditions. Our visualization results show that the critical heat flux around wire heater could be explained by Gorter-Mellink equation taking into account of the Van der Waals pressure [2, 3]. The values are consistent with the microgravity experiment using parabolic flight [5] and also consistent with the prediction from the earth gravity experiments [2, 3, 5]. On the other hand, the heat transfer mechanism across the vapor-liquid interface is still unknown because the vapor sheaths around the heater wire were too large compared with the optical window of 25 mm in diameter, and the large vapor sheath could not avoid the edge effect despite that the heat flux is slightly higher than the critical heat flux. Thus, a steady heat transfer was not realized in this study.

In the previous experiment, bubble collapsing was observed when the wire heater was switched off under microgravity [2]. The images of the collapse show complicated transitional motion and deformation of bubbles, making it hard to analyze. We could roughly analyze only a few data. It was suggested that the visualization experiments of bubble shrinking may show that the heat transfer can be explained by calculating the heat flux across the liquid-vapor interface from the kinetic theory equation.



In this study, we used visualization of the behavior of a single spherical bubble generated by a short wire heater to make a the geometry of a bubble simple. The time variation of the volume of the bubble was calculated based on the data from image analysis. We will also discuss the calculated shrinking speed of the bubble.

2. Experimental setup

2.1. The small cryostat and the drop tower

The small cryostat with optical windows [2 - 4] shown in Figure 1 was used. The cryostat has multi baffles of porous metal plates which have large surface areas to avoid the effect of sloshing flow along the cylinder wall. A LED light and a high speed video camera with a telecentric lens were used for high sensitivity imaging of density distribution. The frame rate was 231 frames/sec. The resolution of images is 1024 x 1024 pixels, corresponding to about 20 $\mu\text{m}/\text{pixel}$. The entire experimental setup, including some measurement devices, a diaphragm pump, and a laptop PC were set inside the capsule in the size of 0.72 m in diameter, 0.82 m in height, and mass less than 60 kg. The 10 m drop tower that was used to obtain the microgravity environment is shown in Figure 2. It is located at the Hokkaido division of National Institute of Advanced Industrial Science and Technology (AIST) in Japan. Due to the double capsule system, the quality of microgravity achieved less than 1 milli-g, for about 1.3 seconds. The small cryostat equipped with optical windows and the entire equipment was dropped more than 100 times.

The residual background flow in the measurement area under microgravity was measured with the PTV (Particle Tracking Velocimetry) technique. Small bubbles in He I, as shown in Figure 3, were regarded as tracking particles for the PTV analysis. The back ground flow velocity depending on the level of liquid helium was found always below 0.1 mm/s. Thus the effects of sloshing and slight vibrations caused by the magnet separation at the start of the free fall are negligibly small.

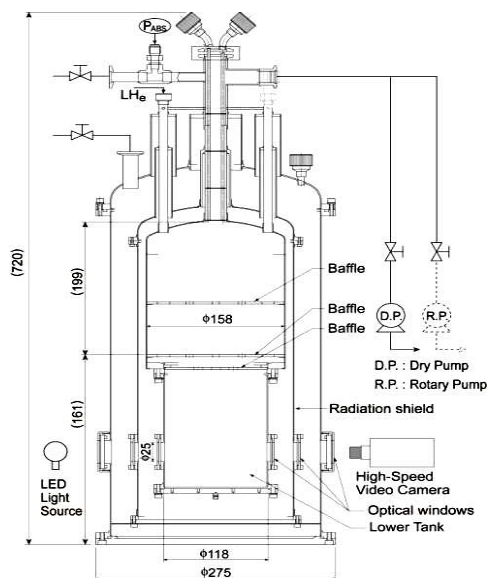


Figure 1. Sketch of the small cryostat cited from [2, 3, 4]

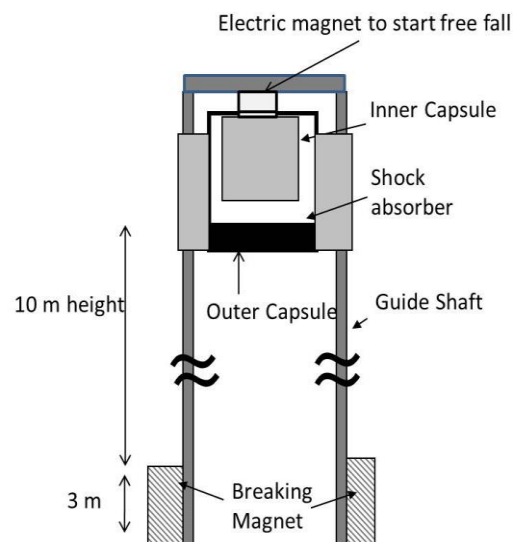


Figure 2. Schematic illustration of the drop tower cited from [1-4]

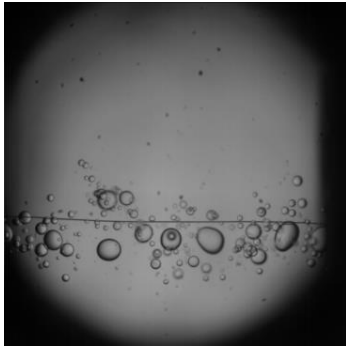


Figure 3. Typical image of tracer bubbles in He I

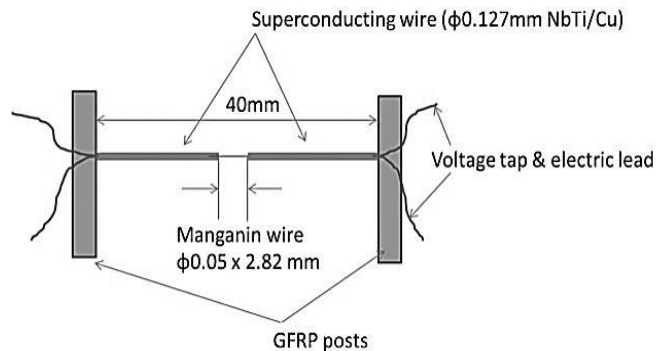


Figure 4. Schematic illustration of the heater unit configuration cited from [4]

2.2. Micro heater unit

The micro heater unit was used as shown in Figure 4, which is the same as in our previous work [3]. A manganin wire, 0.05 mm in outer diameter and 2.82 mm in length, is used as a heater. Two short cooper-stabilized mono-filament NbTi superconducting (SC) wires are connected to the manganin heater. Most of the heat is generated by the manganin wire even when the superconducting wires were quenched due to the copper/SC ratio of 1.6. To make a large spherical bubble of about 10 mm diameter, a constant current was supplied for a duration of 0.4 sec after the free fall start. The bubble shrinking was then visualized after the heater was switched off. Manganin has a strong correlation with temperature in the cryogenic temperature range. Thus, the heater temperature was calculated by the resistance-temperature curve. It should be noted that the heater temperature was measured during vapor growth only.

3. Result and Discussion

Typical visualization results of the bubble behavior are shown in Figures 5 (a)-(h). Figures 5(a) to (d) show the vapor growth during a constant heat generation of 18.05 mW. Figures 5 (e) to (h) show the vapor shrinking after the heater was switched off. In the early stage of vapor growth, the vapor bubble rapidly grew accompanying with oscillation is seen when the bubble size was similar to heater length. After the bubble growth to a rather large bubble, the bubble shape became almost spherically symmetric. It switched to the vapor shrinking phase shortly after the heater was turned off. When the vapor bubble became small, the vapor bubble easily flows and the bubble shape was no longer a perfect sphere.

Figure 6 shows the time variation of the volume of the vapor bubble from the image analysis. The volume was calculated from the shadow area of an assumed perfect sphere. These time variation data indicate two characteristic features. First, the volume of a bubble is proportional to the heat input at the instant of heater switched off. This feature was discussed in the previous paper [4]. And secondly the shrinking speed is depending on the bubble size. Figure 7 is the replotted figure of Figure 6 for shrinking state when $t = 0$ was redefined the moment of vanishing vapor. The time variations of volume are independent of the initial condition of size and heat input. Figure 7 also includes the data of the past experiment [2]. In Figure 7, the plot of the past experiment was taken by the image of vapor shrinking from large vapor sheath which is created by heater of 40 mm manganin wire. The different results have same slope. It seems the bubble volume is determined as a function only of the time until bubble disappearance. The vapor motion and gas condition inside a bubble has no significant effect to the bubble shrinking. Actually, the gas density inside bubble must be depending on the heat input. The heater temperature was found to vary between about 50 and 80 K. These results indicate two possibilities. First, the thermal contraction of gas inside bubble may be rather small. Secondly, the average temperature of gas inside a bubble is almost same in every case as

long as temperature of surrounding He II is the same though the temperature of small heater depends on the heat inputs.

The average temperature of gas inside a bubble is roughly estimated in the following process. First, the heater temperature was calculated on the basis of the relation between the temperature and the resistance. The calculated heater temperature is regarded as the average temperature of the centre sphere of the diameter of 2.82 mm which is the heater length. If a quasi-steady heat conduction from the point heat source is assumed, the average temperature is calculated from the equation of thermal conduction equation for spherical symmetric configuration.

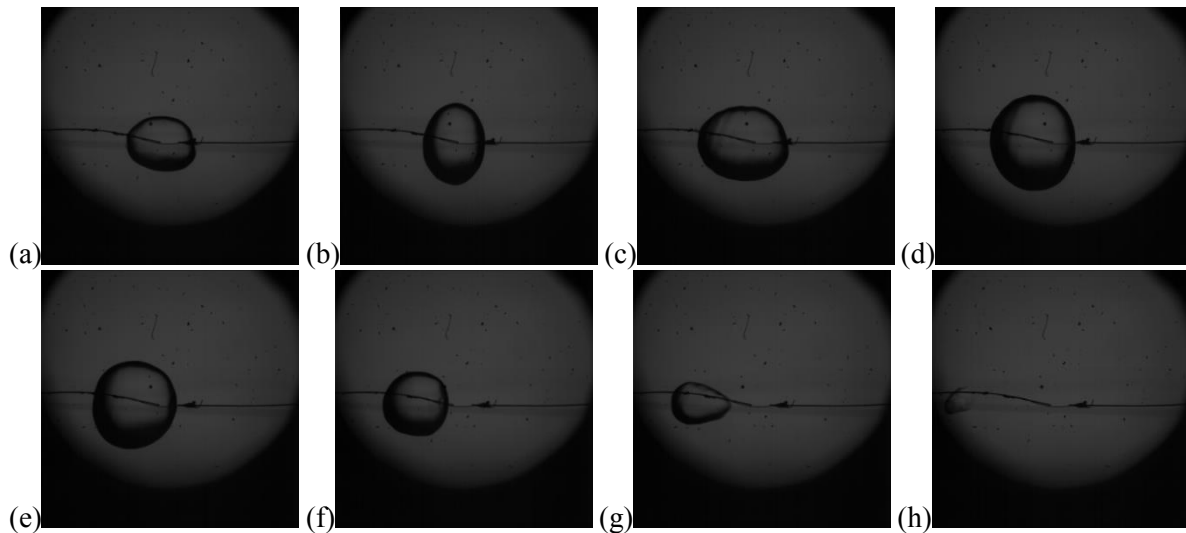


Figure 5. (a)-(h) A typical series of pictures of the growth and shrinking of a single bubble in He II under microgravity heated with 18.05 mW at 1.9 K (a) 0.089 s, (b) 0.193 s, (c) 0.297 s, (d) 0.401 s, (e) 0.504 s, (f) 0.608 s, (g) 0.712 s, and (h) 0.816 s

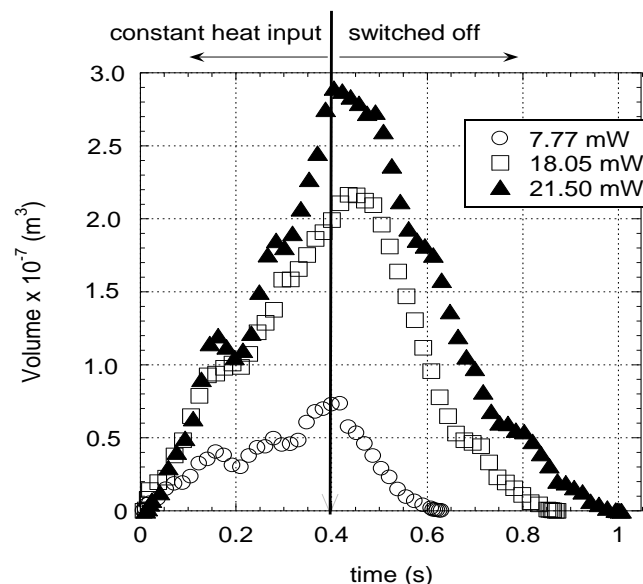


Figure 6. Time variations of bubble volume on several heat input for 0.4 sec at the bath temperature $T_b = 1.9$ K, $t = 0$ is the moment when heater switched on.

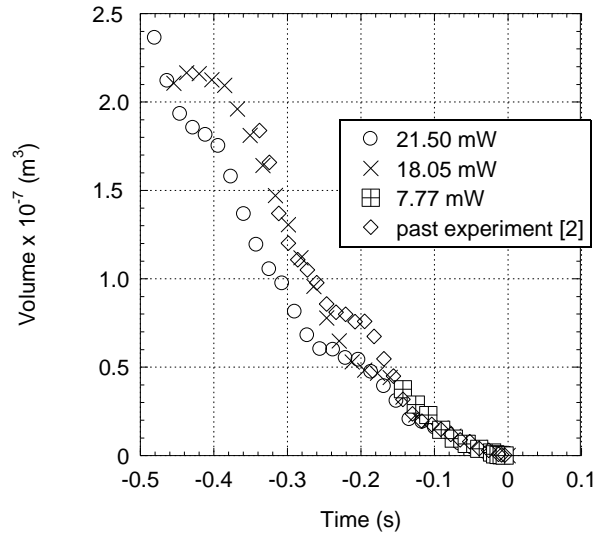


Figure 7. Time variation of the bubble volume during shrinking. $t = 0$ is redefined as the moment of vanishing vapor.

$$Q = 4\pi r^2 \kappa \frac{dT}{dr} \quad (1)$$

$$T_r = T_c + \frac{Q}{4\pi\kappa} \left(\frac{1}{r} - \frac{1}{\varepsilon} \right) \quad (2)$$

$$T_{ave} = \frac{\int_0^{r_i} \left(T_c + \frac{Q}{4\pi\kappa} \left(\frac{1}{r} - \frac{1}{\varepsilon} \right) \right) \cdot 4\pi r^2 dr}{\frac{4}{3}\pi r^3} = T_c + \frac{Q}{4\pi\kappa} \left(\frac{1}{(2/3) \cdot r} - \frac{1}{\varepsilon} \right) \quad (3)$$

In equation (2), ε is the small length assumed. The boundary condition is $T = T_c$ at $r = \varepsilon$. T_c is the temperature of centre of bubble. Corresponding to this consideration, the average temperature of the heater could be regarded as the temperature on the surface of sphere in the diameter of 1.88 mm which is 2/3 of heater length. And then the average thermal conductivity of the bubble was calculated in term of the diameter of bubble, the heat input and the heater temperature approximated by the temperature on the surface of the centre sphere with the diameter of 1.88 mm. The equation is

$$\kappa_{avg}(T_{avg}) = \frac{Q(r_i - r_w)}{4\pi r_i r_w (T_w - T_i)} \quad (4)$$

Here the subscripts w and i mean the location of the heated surface and the liquid-vapor interface respectively. Finally, the average temperature inside the bubble was estimated by the relation between this calculated averaged thermal conductivity and the properties of helium gas [6]. These rough estimations of gas temperature inside bubble were between 5 and 7 K. These estimated temperatures were used in following discussion.

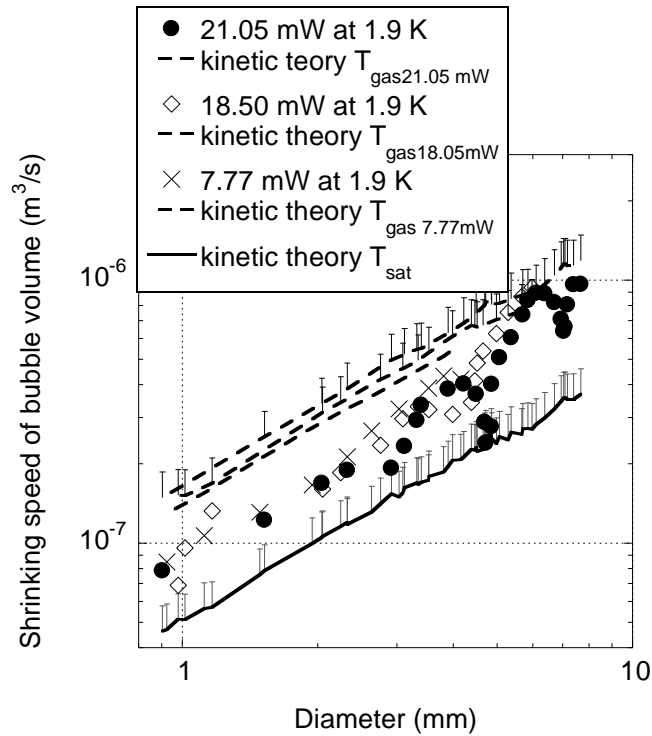


Figure 8. Shrinking speed of the vapor bubble at $T_b = 1.9$ K compared with the calculations based on the kinetic theory.

Figure 8 shows the shrinking speed of the volume, which is the derivative of the time variation in Figure 7. It is fair to describe that the shrinking speed is roughly proportional to the diameter. In other words, the heat flux across liquid-vapor interface must be proportional to the reciprocal of the diameter. In figure 8, the solid line and the dashed line were drawn based on the equation of energy balance in non-equilibrium state of two phases based on the linear kinetic theory [7-9]. The equation of energy balance is

$$2\sqrt{\pi}\left(\frac{1-0.4\beta}{\beta}\right)j - \Delta p\sqrt{2RT_i} + \frac{\sqrt{\pi}}{4}q_i = 0 \quad (5)$$

where j is the mass flux across the interface, β the thermal expansion ratio, q_i the heat flux across interface, and T_i the temperature at the interface (not the bath temperature). In this study, the approximation $T_i = T_b$ is used because it is assumed that the temperature difference is quite small because of the small heat flux [10]. We use measurement speed of interface motion for j and $\beta = 0.72$ referred from a previous paper [11]. Actually the absolute value of the first term is less than 1/10 of that of the second term so that this experiment is performed not in a highly transient state from the point of view of linearized kinetic theory. In the past reports [7-9], the term of pressure difference Δp was the sum of the pressure head on the interface and surface tension. In the microgravity experiment, Δp should be only the surface tension so that the equation 5 is rewritten as follows.

$$2\sqrt{\pi}\left(\frac{1-0.4\beta}{\beta}\right)j - \frac{4\sigma}{D}\sqrt{2RT_i} + \frac{\sqrt{\pi}}{4}q_i = 0, \quad (6)$$

where D is the diameter and σ is the surface tension. Thus the heat flux q_i can be calculated by

$$q_i = \frac{4}{\sqrt{\pi}}\left(\frac{4\sigma}{D}\sqrt{2RT_i} + 2\sqrt{\pi}\left(\frac{1-0.4\beta}{\beta}\right)j\right) \quad (7)$$

The speed of vapor shrinking dV/dt is calculated from the equation using q_i

$$\frac{dV}{dt} = \frac{\pi D^2 q_i}{\rho h_{fg}} \quad (8)$$

where ρ is the gas density and h_{fg} the latent heat. In the Figure 8, the solid line shows the results calculated with the gas density of the vapor bubble estimated by the saturated vapor pressure, while the dashed line shows the results using with the gas density of the estimated average temperature. The bubbles were not perfect spheres so that the surface areas were estimated smaller than the actual areas. The error bars were drawn with +25 % that is the maximum ratio between the shadow area of the bubble and peripheral length of it. When the diameter of a bubble became small, the calculation and measurement results were getting closer. On the other hand when the vapor bubble is rather large, the measured shrinking speed of bubble volume is close to the calculation result drawn by the dashed line. In this study, the specific heat of gas has not been taken into account because it is negligibly small compared to the latent heat in this experiment. It could be considered that the temperature of gas inside the bubble was getting lower and the gas inside the bubble slowly approached to that on the saturated line. The result may be summarized as follows on the basis of the comparison between the experimental data and the theoretical treatment: For small diameter of a bubble the phenomena can be described by the theory with the gas density estimated in terms of the average temperature as indicated by the solid line. For large diameter the phenomena can be described by the theory with the gas density estimated along the saturated vapour pressure as indicated by the dashed line. In fact, the diameters of most experimental data are in the transition regime between the two limiting cases. Thus, it can be concluded that the shrinking speed of bubble is represented by heat transport as explained by the kinetic theory and gas constriction. These discussions assume the system is in quasi-steady state. Thus the measurement data are all between the calculated two lines. Furthermore, the numerical simulation with a moving interface and the equations of bubble dynamics should be possible to make a precise prediction calculation for these transient phenomena.

In addition, it should be emphasized that the Van der Waals pressure is not included in the above equations. Van der Waals pressure plays a dominant role for critical heat flux in microgravity [2, 3, 5], but after macroscopic vapor generation, only the surface tension plays a crucial role to heat transport across the liquid-vapor interface. The Van der Waals pressure is about 80 Pa. On the other hand, the pressure difference due to surface tension is about 0.1 Pa for a bubble diameter of 10 mm. Satisfactory agreements with the kinetic theory is also observed at the other bath temperatures of 2.1 and 2.15 K as shown in Figure 9 and 10. These results show that this phenomenon does not depend on the difference between the bath and the lambda temperature. Thus, this phenomenon must be independent with superfluidity. However, in ordinary fluid this kind of experiment may be difficult because the vapor density is much higher than for He II and the ideal temperature distribution of the liquid phase is not easy to be realized in ordinary fluid. The temperature variation throughout He II is negligibly small due to extremely high effective thermal conductivity so that the ideal situation of temperature uniformity for kinetic theory was in fact realized.

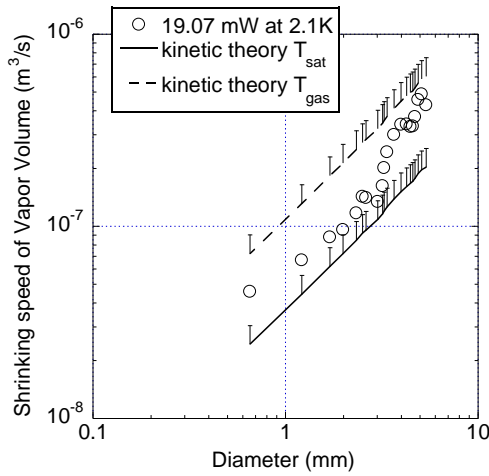


Figure 9. Shrinking speed of the vapor bubble at $T_b = 2.1$ K compared with the calculations based on kinetic theory.

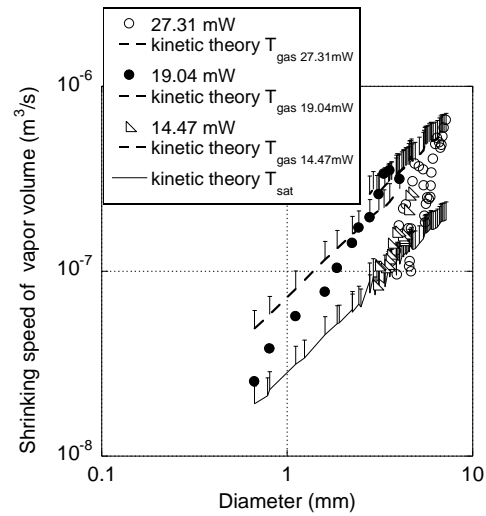


Figure 10. Shrinking speed of the vapor bubble at $T_b = 2.16$ K compared with the calculations based on kinetic theory.

Here, we examined how far the present experiment was from the steady state. The steady diameter of the bubble should be calculated by using this heat transport mechanism. When the steady state $dV/dt = 0$ is reached, the theoretical heat transport and heat transport across the interface are expressed by the following equations:

$$q_i = \frac{4}{\sqrt{\pi}} \left(\frac{4\sigma}{D} \sqrt{2RT_i} \right) \quad (8)$$

$$Q = q_i D^2 \pi \quad (9)$$

These simultaneous equations can be solved. The solution for the diameter of steady state is calculated by the following equation.

$$D = Q / 16\sigma \sqrt{2RT_i \pi} \quad (10)$$

Figure 11 shows the calculation results of Equation 10 and the measurement result of the diameter at 1.2 sec after the onset of heating. 1.2 sec is the longest time duration of microgravity in this experimental setup. It is seen in Figure 12 that bubbles still keep growing. The difference between the calculated and measurement results is getting larger when heat input becomes large. To verify this discussion, the experiment of steady heat transfer across liquid-vapor interface needs much more time duration of microgravity environment.

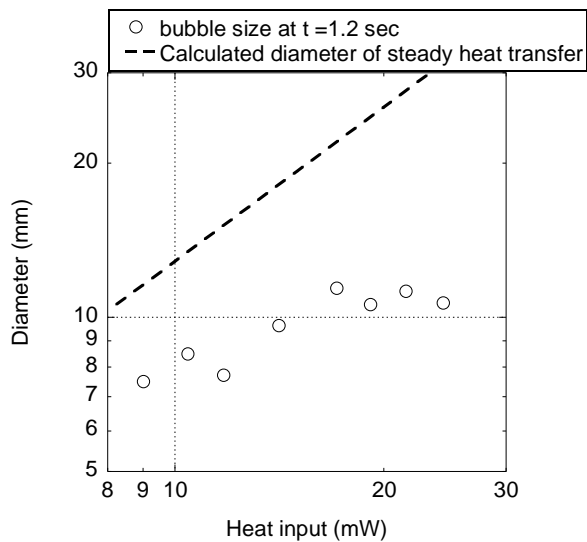


Figure 11. Calculated the diameter of steady state and the measurement results 1.2 s after heating start at 1.9 K

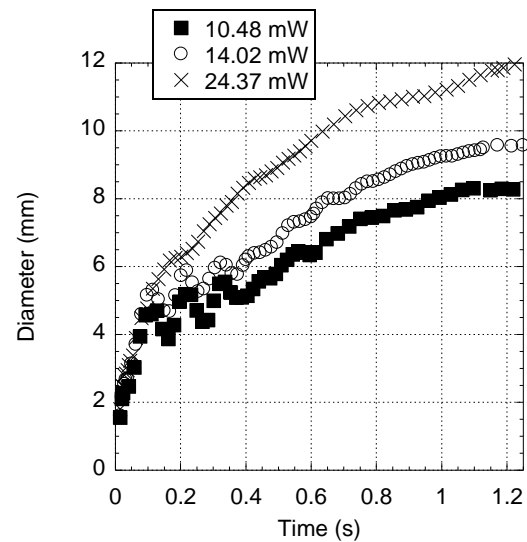


Figure 12. Time variation of the volume of the vapor bubble for the several heat inputs in He II at 1.9 K. (replotted figure cited)

4. Conclusion

To investigate the heat transfer across liquid-vapor interface under microgravity condition, the visualization experiment of shrinking single bubble were carried out with the drop tower. Image analyses of taken picture by the high speed video camera reveal the followings.

- The shrinking speed of bubble under microgravity condition is represented the heat transport explained by the kinetic theory and the gas constriction.
- The pressure difference due to surface tension plays role to heat transfer across liquid-vapor interface in microgravity. The Van der Waals pressure plays role to only critical heat flux of onset boiling.
- The bubble size of steady state for heat input was predicted. It takes much more time duration than 1.2 sec to reach steady state.

Acknowledgement

This research was financially supported by a Grant-in-Aid for Scientific Research from the Japan Society for the Promotion of Science (Grant No.2528289300). We thank to Mikito Mamiya and Hideaki Nagai at AIST for their help with the operation of the drop tower.

References

- [1] Kimura N., Takada S. et al, 2011, *Cryogenics*, 51 p 74-78 (Amsterdam Elsevier)
- [2] Takada S., Kimura N. et al., 2014, *Advances in Cryogenics Engineering*, 59A p 292-299 (New York, AIP publishing)
- [3] Takada S., Kimura N., Mamiya M., Nagai H., Murakami M., Okamura T. and Nozawa M., 2014 *Int. J. Microgravity Sci. Appl.* Vol. 31 No. 4 p 1-2 (in Japanese) (Saitama The Japan Society of Microgravity Application)
- [4] Takada S., Kimura N., Mamiya M., Nagai H. and Murakami M., Visualization Study of Growth of Spherical Bubble in He II Boiling under Microgravity Condition, physics procedia, Proceedings of ICEC25-ICMC2014 in press (Amsterdam Elsevier)

- [5] Gradt T., Szücs Z., Denne H. D. and Klipping G., 1986 *Advances Cryogenics Engineering* vol 31 p 499-504 (New York and London, Plenum Press)
- [6] Arp V., HEPAK, Cryodata
- [7] Ametitov Y., 1983 *Cryogenics* **23** p 179-184 (Amsterdam Elsevier)
- [8] Kryukov A. P., van Sciver S. W., 1981 *Cryogenics* **21** p 525-528 (Amsterdam Elsevier)
- [9] D. A. Labuntzov and Y. Ametitov, 1979 *Cryogenics* **19** p 401-404 (Amsterdam Elsevier)
- [10] Jebali F., Francois M.X., 1994 *Physica B* 194-196 p. 599-600 (Amsterdam Elsevier)
- [11] Murakami M., Furukawa T., Maki M., Fujiyama J., 2002 *Experimental Thermal and Fluid Science*, Volume 26 p 229-235 (Amsterdam Elsevier)